TAO, Vol.5, No.2, 121-136, June 1994

Convection and Mei-Yu Front

HAN-RU CHO[1] and GEORGE T. J. CHEN[2]

(Manuscript received 10 January 1994, in final form 18 May 1994)

ABSTRACT

The genesis of Mei-Yu fronts is studied by assuming the fronts are characterized by a line of low-level potential vorticity (PV) anomaly. It is proposed that the frontogenetic process is initiated by the CISK mechanism through the interactions between the PV anomaly and the convection induced by Ekman layer pumping. The scale contraction produced by the convergence flow of the convection provides the basic frontogenetic forcing. In addition, the cross-frontal horizontal scale of the front contracts at a rate faster than what can be expected from a linear theory, due to the presence of a nonlinear feedback process. The process is due to the fact that the effect of condensation on PV is proportional to the value of absolute vorticity. These processes are illustrated using both a linear analysis and a nonlinear munerical model.

(Key words: Potential vorticity, Mei-Yu frontogenesis, Scale contraction, Nonlinear process, Cumulus heating)

1. INTRODUCTION

Mei-Yu fronts occur in the subtropical Asia in the transition period between the dry northeast and moist southwest monsoons. They form in the region between a migratory high to the north and the subtropical Pacific high to the south. Unlike the fronts associated with midlatitude cyclones observed in North America or Europe, they move only slowly southeastward during the early stage of their lifetimes, and appear as a quasi-stationary front at the later stage.

There have been many studies of Mei-Yu fronts (Chen, 1977, 1983, 1988, 1990, and 1991; Chen and Jou, 1988; Chen and Tsay, 1978). A special field project TAMEX was conducted in 1987 (Kuo and Chen, 1990) to study their mesoscale features (e.g. Trier, *et al*, 1990). The properties of Mei-Yu fronts appear to vary during different periods of the season, and even from sector to sector along the fronts. Chen and Chang (1980) noted that the eastern and central sections of Mei-Yu fronts near Japan and over the East China Sea resemble the well known midlatitude baroclinic fronts, whereas the western section over

[1] Department of Physics, University of Toronto, Toronto Ontario, Canada

[2] Department of Atmospheric Sciences, National Taiwan University, Taipei, Taiwan, R.O.C.

southern China resembles semitropical disturbances with an equivalent warm core structure, a weak horizontal temperature gradient, and a strong horizontal wind shear in the low levels, all evidences of the presence of a low-level potential vorticity (PV) maximum.

The precipitation along Mei-Yu fronts in Southern China and Taiwan is mostly produced by deep convective clouds. From 25 cases of Mei-Yu fronts occurred over southern China during 1981-85, Chen and Jou (1988) concluded that the amount of convection is independent of the presence or absence of any appreciable baroclinicity. The only factor which has a strong influence is the moisture content of the low level air slightly to the south of the fronts. If moderately strong southwesterly flow carries warm and moist air into the region from the Bay of Bengal, convective activities tend to be very strong. On the other hand, if the subtropical Pacific high induces southeasterly to southwesterly flow carrying air into the region from the Pacific, only average to weak convection can be expected.

The independence of the strength of convection on the presence or absence of large scale forcing such as appreciable cross front temperature contrast poses a rather interesting question: What are the processes responsible for the frontal characteristics over the southern and western portions of Mei-Yu front? How are the convective activities along Mei-Yu fronts maintained, other than an abundant moisture supply? We shall attempt to address these questions in this paper. Two positive feedback processes are proposed as responsible for the frontal characteristics of Mei-Yu fronts over south China, the first being the classical linear CISK process, and the second a nonlinear process.

The possible presence of a low-level PV anomaly has several effects on the development of the front. First, the large wind shear across the anomaly can induce convergent flow by boundary layer processes. This is the classical CISK mechanism which tends to induce convection, the heating from which further enhances low-level potential vorticity anomaly. It is a positive feedback loop which can initiate the Mei-Yu frontal development and the associated precipitation.

Secondly, as can be seen from the potential vorticity equation, the effect of condensational heating on PV depends on the value of vorticity; the larger the value of vorticity, the stronger is the effect. A low level PV anomaly means increased vorticity both within and above the anomaly, and hence an increased effect of condensational heating on low-level potential vorticity, This is a nonlinear enhancement of the CISK process, and the development of Mei-Yu fronts will be enhanced because of this nonlinear feedback.

This dependence of the effect of condensational heating on background vorticity value can be understood from two slightly different viewpoints, one from the point of view of vorticity dynamics, the other from the thermodynamic equation. First, heating induces upward motion and the associated low-level convergence and upper-level divergence. The effect of convergence/divergence on the vorticity field is proportional to vorticity itself. Since potential vorticity can be viewed as vorticity on isentropic surfaces, the effect of heating on the PV field should therefore be proportional to vorticity.

The second viewpoint was first pointed out by Schubert and Hack (1986). The strength of ageostrophic flow, while proportional to forcing, is inversely proportional to inertial stability which is proportional to absolute vorticity. Other factors being equal, larger values of vorticity means weaker ageostrophic circulation, and therefore, more of the heat released will be transformed locally into the internal energy of air, and thus enhancing the effect of heating on potential vorticity. As far as balanced flows are concerned, this second interpretation is equivalent to the first because the vorticity field and the temperature field are related through the balance condition.

From these discussions it seems that Mei-Yu frontal development is the result of two positive feedback mechanisms related to the low-level PV anomaly. In this sense, Mei-Yu fronts may be identified as lines of positive low-level PV anomaly. The details of these processes will be examined further after a brief discussion of the model equations to be used in this study.

2. MATHEMATICAL MODEL

For the purpose of illustration, the mathematical model used in this study will include only physical processes we consider to be essential for the Mei-Yu frontogenesis. Therefore the results obtained from the model will be correct only qualitatively. The assumptions made include the following: (1) Mei-Yu front is parallel to the y-axis with a two dimensional structure in the (x, z) plane; (2) the Boussinesq approximation will be made and the Coriolis parameter f will be assumed constant; (3) heat and momentum fluxes due to small scale turbulent eddies are confined to the atmospheric boundary layer the top of which coincides with the base of cumulus clouds; (4) The effect on the thermodynamic equation of the sensible heat flux in the boundary layer will be neglected. This approximation is not always supported by observations as the sensible and latent heat fluxes are generally important in the vicinity of Mei-Yu fronts. The assumption is made because the effect is not an essential part of the processes we are going to discuss; (5) the surface layer where very large wind shear exists due to friction at the surface is very shallow so that its depth δ_s can be assumed to be zero. This assumption can usually be justified because $\delta_s \sim 0.1 \times \delta_b$ where δ_b is the depth of the boundary layer, (6) along-front geostrophy is an adequate approximation above the surface layer. A similar approximation is made, for example, in Thorpe and Nash (1986).

Assumptions (3)-(6) are concerned with our specific treatment of the boundary layer. Some authors attempted to avoid the difficulty introduced by the boundary layer by assuming that the bottoms of their models are located at the top of the boundary layer. Had we made the same assumption, we would obtain qualitatively the same results as what we are going to present here. Because of (6), the geostrophic momentum approximation can be adopted and the geostrophic coordinate used:

$$X = x + \frac{v_g}{f}, \quad Z = z$$

where v_g is the y-component of the geostrophic wind, and (X, Z) and (x, z) are the geostrophic and the physical coordinates, respectively. Following Hoskins and Bretherton (1972) and Hoskins (1975), the governing equations in the geostrophic coordinates can be written as:

$$\begin{aligned} f v_g &= -\frac{\partial \phi}{\partial X} \\ \frac{D v_g}{D t} + f u_a &= \frac{\partial \tau_v}{\partial Z} \\ \frac{D \theta}{D t} &= E \end{aligned} \tag{1}$$

$$\frac{\partial u}{\partial X} + \frac{\partial w}{\partial Z} = 0$$

where u_a is the X component of the ageostrophic wind, ϕ is the geopotential, τ_v the y-component of the turbulent momentum flux in the boundary layer, and E the rate of heating due to latent heat release in cumulus clouds. In the geostrophic coordinate

$$\frac{D}{Dt} = \frac{\partial}{\partial t} + u_g \frac{\partial}{\partial X} + w \frac{\partial}{\partial Z}$$

u_g here is the X component of the geostrophic wind. Equivalently, the prognostic equations for θ and v_g can also be written in terms of the potential temperature and the geostrophic potential vorticity defined as $q = \zeta(\partial\theta/\partial Z)$ where ζ is the Z component of the absolute geostrophic vorticity:

$$\frac{D\theta}{Dt} = E, \quad \frac{Dq}{Dt} = \zeta \frac{\partial E}{\partial Z} + \frac{\partial \theta}{\partial Z} \frac{\partial^2 \tau_v}{\partial Z \partial X}$$

Here one further approximation will be made that (7) the generation of potential vorticity due to turbulent friction above the surface layer is small and can be neglected in comparison with the generation due to latent heating. This assumption can be justified so long the vertical wind shear in the boundary layer take place mostly within the surface layer. A justification of this can be found in Appendix The extent to which the atmospheric flow is influenced by the boundary-layer PV is an interesting problem in its own right and is beyond the scope of this investigation. With this approximation, the equations become

$$\frac{D\theta}{Dt} = E, \quad \frac{Dq}{Dt} = \zeta \frac{\partial E}{\partial Z} \tag{2}$$

From the definition of potential vorticity, an equation can be derived relating the distribution of potential temperature to the distribution of potential vorticity:

$$\frac{1}{f^2} \frac{\partial^2 \theta}{\partial X^2} + \frac{\partial}{\partial Z}\left(\frac{f\theta_0}{gq} \frac{\partial \theta}{\partial Z}\right) = 0 \tag{3}$$

provided that the values of θ at the boundaries are given. Because of the existence of the geostrophic balance, v and θ is not independent. The transverse circulation implied by the equations in (1) is given by

$$f^2 \frac{\partial^2 \psi}{\partial Z^2} + \frac{g}{f\theta_0} \frac{\partial}{\partial X}\left(q \frac{\partial \psi}{\partial X}\right) = 2 \frac{g}{\theta_0} \frac{\partial u_g}{\partial X} \frac{\partial \theta}{\partial X} - \frac{g}{\theta_0} \frac{\partial E}{\partial X} + f \frac{\partial^2 \tau_v}{\partial Z^2} \tag{4}$$

where ψ is the stream function in the physical space (x, z) plane, while the circulation equation is written in the geostrophic space (X, Z). The vertical velocity is thus given by $w = -(\partial\psi/\partial x) = -(\zeta/f)(\partial\psi/\partial X)$. u_g will be assumed to be zero in this analysis. (4) then implies that the stream function can be decomposed into two components:

$$\psi = \psi_h + \psi_e$$

with the first component associated with the heating due to latent heat release

$$f^2\frac{\partial^2\psi_h}{\partial Z^2}+\frac{g}{f\theta_0}\frac{\partial}{\partial X}(q\frac{\partial\psi_h}{\partial X})=-\frac{g}{\theta_0}\frac{\partial E}{\partial X} \tag{5}$$

and the second component associated with eddy viscosity

$$f^2\frac{\partial^2\psi_e}{\partial Z^2}+\frac{g}{f\theta_0}\frac{\partial}{\partial X}(q\frac{\partial\psi_e}{\partial X})=f\frac{\partial^2\tau_v}{\partial Z^2}$$

We will not attempt to solve this equation by specifying the vertical structure of the eddy momentum flux. Instead it will suffice to assume that at the top of the boundary layer the viscosity-induced vertical velocity is given according to the Ekman layer theory (Holton,1992):

$$w_e^*=k_e\zeta_r^*=(K/2f)^{1/2}\zeta_r^* \tag{6}$$

where K is the coefficient of eddy viscosity and $k_e=(K/2f)^{1/2}$. ζ_r is the relative vorticity and the asterisks denote values evaluated at the top of the boundary layer. The model used in our analysis consists of equations (2)-(6).

3. LINEAR ANALYSIS

CISK analyses are often made for tropical systems. For midlatitude systems, CISK is usually discussed in baroclinically unstable systems. A linear CISK analysis is made here to demonstrate that CISK may be responsible for the initiation of Mei-Yu frontogenesis. To illustrate the independence of the formation of Mei-Yu front on background baroclinity, we will assume that the background state of the analysis is homogeneous in X with a constant vertical gradient in θ:

$$\theta=\bar{\theta}(Z),\quad \zeta=\bar{\zeta},\quad q=q_0=\bar{\zeta}\frac{\partial\bar{\theta}}{\partial Z}$$

The atmosphere is assumed stationary at the initial time except a small perturbation proportional to

$$e^{\sigma t}e^{ikX}$$

We will examine the properties of σ, how it depends on the wavenumber k and other background parameters. In the following a buoyancy frequency N will be used which is defined as

$$N^2=\frac{g}{\theta_0}\frac{q_0}{f}$$

The governing equations for the perturbation quantities can be obtained by linearizing (2) through (6):

$$\frac{\partial q'}{\partial t}=f\frac{\partial E'}{\partial Z} \tag{7a}$$

$$\frac{1}{f^2}\frac{\partial^2\theta'}{\partial X^2}+\frac{1}{N^2}\frac{\partial^2\theta'}{\partial Z^2}=\frac{1}{fN^2}\frac{\partial q'}{\partial Z} \tag{7b}$$

$$f^2\frac{\partial^2\psi_h'}{\partial Z^2}+N^2\frac{\partial^2\psi_h'}{\partial X^2}=-\frac{g}{\theta_0}\frac{\partial E'}{\partial X} \tag{7c}$$

with the vertical velocity at the top of the boundary layer induced by eddy viscosity given by

$$w_e^*=k_e\zeta'^*=(K/2f)^{1/2}\zeta'^*$$

The primed variables denote deviatins from the background state. A simple parameterization will be used to represent cumulus heating:

$$E=\epsilon w^* h(Z) \tag{8a}$$

where $h(Z)$ gives the vertical distribution of heating. A piecewise linear profile will be used

$$h(Z)=\begin{cases}\frac{2}{H}\frac{Z}{Z_p} & Z<Z_p\\ \frac{2}{H}\frac{H-Z}{H-Z_p} & Z>Z_p\end{cases} \tag{8b}$$

$h(Z)$ is normalized in the sense that the vertical integration of $h(Z)$ from the lower to the upper domain boundary gives unity.

The solution to the linear eigenvalue problem can be obtained in a straightforward manner. First consider (7c), we note after assuming sinusoidal variation in X it can be written as

$$\frac{\partial^2\psi_h'}{\partial Z^2}-\frac{N^2k^2}{f^2}\psi_h'=-i\frac{kg}{f^2\theta_0}E'$$

Decomposing the stream function into a particular and complimentary part

$$\psi_h'=\psi_p'+\psi_c'$$

and letting

$$\psi_p'=i\frac{g}{\theta_0}\frac{1}{N^2k}E'$$

one gets

$$\frac{\partial^2\psi_c'}{\partial Z^2}-\frac{N^2k^2}{f^2}\psi_c'=-\frac{\partial^2\psi_p'}{\partial Z^2}=i\frac{g}{\theta_0}\frac{\epsilon w'^*}{N^2k}\frac{2\delta(Z-Z_p)}{Z_p(H-Z_p)}$$

where δ is the Dirac delta function. ψ_c' is therefore the Green function of the above equation and is given by

$$\psi_c' = -i\frac{g}{\theta_0}\frac{\epsilon w'^*}{N^2 k}\frac{f}{Nk}F(Z)$$

where

$$F(Z) = 2[Z_p(H-Z_p)]^{-1}[\coth\frac{Nk}{f}(H-Z_p) + \coth\frac{Nk}{f}Z_p]^{-1}$$

$$\times \begin{cases} \sinh\frac{Nk}{f}Z/\sinh\frac{Nk}{f}Z_p & Z < Z_p \\ \sinh\frac{Nk}{f}(H-Z)/\sinh\frac{Nk}{f}(H-Z_p) & Z > Z_p \end{cases}$$

Therefore

$$\psi_h' = i\frac{g}{\theta_0}\frac{\epsilon w'^*}{N^2 k}G(Z) \tag{9a}$$

and

$$G(Z) = h(Z) - \frac{f}{Nk}F(Z) \tag{9b}$$

To obtain the solution for the perturbation potential temperature, we note after combining (7a) and (7b)

$$[\frac{1}{f^2}\frac{\partial^2}{\partial X^2} + \frac{1}{N^2}\frac{\partial^2}{\partial Z^2}]\frac{\partial\theta'}{\partial t} = \frac{1}{N^2}\frac{\partial^2 E'}{\partial Z^2}$$

which becomes after substituting (8)

$$[\frac{\partial^2}{\partial Z^2} - \frac{N^2k^2}{f^2}]\theta' = -\frac{1}{\sigma}\frac{2\epsilon w'^*}{Z_p(H-Z_p)}\delta(Z-Z_p)$$

where σ is the growth rate. θ' is therefore also the Green function of the equation. Using the boundary condition $\theta' = 0$ at $Z = 0$ and H, one obtains

$$\theta' = \frac{\epsilon w'^*}{\sigma}\frac{f}{Nk}F(Z) \tag{10}$$

where $F(Z)$ is the same as defined earlier. Since no surface heat flux or background baroclinicity is assumed in the analysis, the boundary condition used for θ' appears to be reasonable. Once the perturbation temperature is determined, one can determine the perturbation vorticity from the relation

$$q' = \bar{\zeta}\frac{\partial\theta'}{\partial Z} + \zeta'\frac{\partial\bar{\theta}}{\partial Z}$$

and (7a):

$$\zeta' = [\frac{\partial\bar{\theta}}{\partial Z}]^{-1}\bar{\zeta}\frac{\epsilon w'^*}{\sigma}\frac{\partial G(Z)}{\partial Z} \tag{11}$$

The growth rate σ can be determined by noting that at the top of the boundary layer $Z = Z^*$, the heating induced vertical velocity is given by

$$w_h'^* = -ik\frac{\bar{\zeta}}{f}\psi_h'(Z^*) = \frac{g}{\theta_0}\frac{\epsilon w'^*}{N^2}\frac{\bar{\zeta}}{f}G(Z^*)$$

and ther vertical velocity due to Ekman layer pumping

$$w_e'^* = k_e\zeta'^* = k_e[\frac{\partial\bar{\theta}}{\partial Z}]^{-1}\bar{\zeta}\frac{\epsilon w'^*}{\sigma}\frac{\partial G(Z^*)}{\partial Z}$$

Since $w'(Z^*) = w'^* = w_h'^* + w_e'^*$,

$$1 = \epsilon\frac{\bar{\zeta}}{f}[\frac{g}{\theta_0}\frac{1}{N^2}G(Z^*) + k_e[\frac{\partial\bar{\theta}}{\partial Z}]^{-1}\frac{f}{\sigma}\frac{\partial G(Z^*)}{\partial Z}]$$

We get after rearranging terms:

$$\sigma = \frac{k_e\epsilon\bar{\zeta}^2\frac{\partial G(Z^*)}{\partial Z}}{q_0 - \epsilon\bar{\zeta}G(Z^*)} \tag{12}$$

The growth rate is directly proportional to k_e since the Ekman layer pumping is the controlling mechanism in this analysis. The solid curves in Figure 1 show the growth rate as functions of wavelength, both in logarithmic scale, for three different values of the background absolute vorticity. The calculations were made with the following set of parameter values:

$$f = 0.6 \times 10^{-4}s^{-1}, \quad H = 10km, \quad \theta_0 = 293K, \quad \frac{\partial\bar{\theta}}{\partial Z} = 3K\ km^{-1}$$

$$Z^* = 1km, \qquad Z_p = 5km, \qquad K = 5m^2s^{-1}, \qquad \epsilon = 58K$$

The three curves labelled 1, 2, and 3 correspond to background vorticity

$$\bar{\zeta} = f, \quad \frac{4}{3}f, \quad \frac{5}{3}f$$

respectively. The effect of heating increases with increasing value of background vorticity. The growth rates are rather fast and are remarkably independent of wavelength for wavelength smaller than 1000 km; the e-folding time is substantially less than a day in this range of the spectrum, and is about 0.25 day for curve 2. For wavelength above 1000 km, the growth rates decrease rapidly. The instability produces therefore mainly mesoscale phenomena and the effect of the positive feedback mechanism is not diminished if the scale of the phenomenon decreases with time.

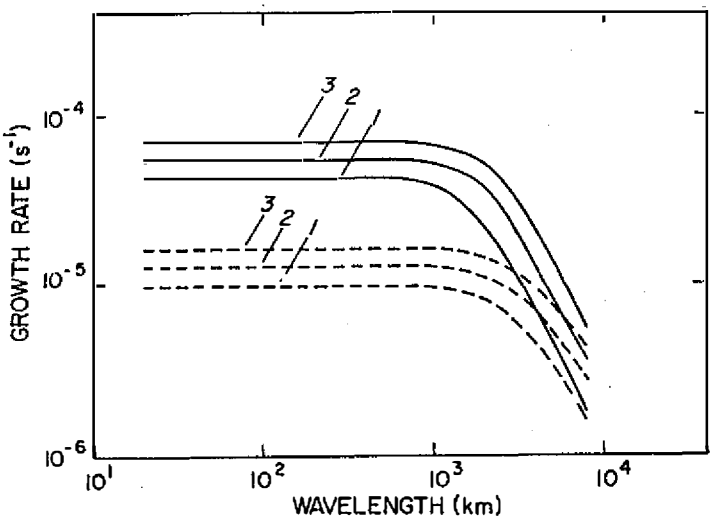

Fig. 1. Growth rate as function of wavelength with and without the contribution from thermally induced boundary layer moisture convergence plotted as solid and dashed curves, respectively. The curves labelled as 1, 2, and 3 corresponds to background absolute vorticity f, $(4/3)f$ and $(5/3)f$, respectively. Values of other parameters are given in the text.

The rapid growth rate indicates that meso-β scale cloud clusters can appear rapidly after some small initial perturbations. The growth rate, as indicated in (12) depends on the value of heating parameter which is proportional to the amount of moisture in the boundary layer. As we will show in the sensitive studies, the growth rate is substantially reduced if the heating parameter is reduced by half.

The scale dependence of the growth rate can be understood from the sturcture of the disturbance. Heating by cumulus clouds goes to driving vertical motion against vertical stability, and to heating the atmosphere and increasing the potential temperature. Since the present CISK mechanism is proportional to the rate of convergence (and therefore vorticity) at the low levels, the growth rate is proportional to the first component, and decreases as the magnitude of the second component increases. Since the effect of this second component is appreciable only when the scale of the disturbance becomes comparable to or larger than the Rossby radius of deformation, the growth rate is more or less independent of wavelength for wavelength less than 1000 km or so.

In our analysis both the frictional induced as well as the thermally induced low-level moisture convergence is included in calculating cumulus heating. The inclusion of this thermally induced component is a major departures from Charney and Eliassen's original CISK analysis (Charney and Eliassen, 1964). In Figure 1, the three dashed curves are the growth rates obtained with this thermal component removed. As can be seen from the figure, the thermally induced low-level convergence provides a major part of the moisture used in cumulus heating, even though frictional induced convergence is the controlling factor in the positive feedback loop.

Because of the simplicity of the model used to describe a rather complex cumulus convection process, it is not easy to estimate the value of the heating parameter ε. If one assumes that total heating is equal to the moisture convergence in the boundary layer, then

$$\varepsilon = \frac{Lr_m}{C_p} \approx 2.5 \times 10^3 r_m$$

where L and C_p are the latent heat of vaporization and the heat capacity at constant pressure, respectively. r_m is the typical specific humidity in the boundary layer. But in reality total latent heat release in an air column is influenced by a number of factors, and could be considerably larger than the amount indicated by boundary layer moisture convergence alone. These factors include surface evaporation which could be quite considerable if strong surface winds are present, and moisture convergence above the cloud base level. Craig and Cho (1988) suggested that a more appropriate vlaue should be

$$\varepsilon = \eta \frac{Lr_m}{C_p}$$

and the values of η estimated from a number of observed polar air stream disturbances range between 2 and 4. Here we adopt the conservative estimate η=2. Using this value we have

$$\varepsilon = \begin{cases} 50K & if \ r_m = 10g\ kg^{-1} \\ 25K & if \ r_m = 5g\ kg^{-1} \end{cases}$$

We present in Figure 2 the growth rates for the same three cases as before, except the heating parameter ε=25 K is used. The growth rates are much smaller than those shown in Figure 1; the e-folding time for curve 2 is about 2.3 days in the mesoscale. A comparison between the solid and the dashed curves in this figure shows the contribution due to heating induced moisture convergence becomes smaller relative to the contribution from friction induced boundary layer convergence, due to the reduced heating rate.

Because of its linear nature, the present analysis does not include the nonlinear feedback process discussed in the introduction, except for the simple demonstration that the growth rate becomes larger with larger background vorticity. The inclusion of this process requires a nonlinear model which will be discussed in the next section.

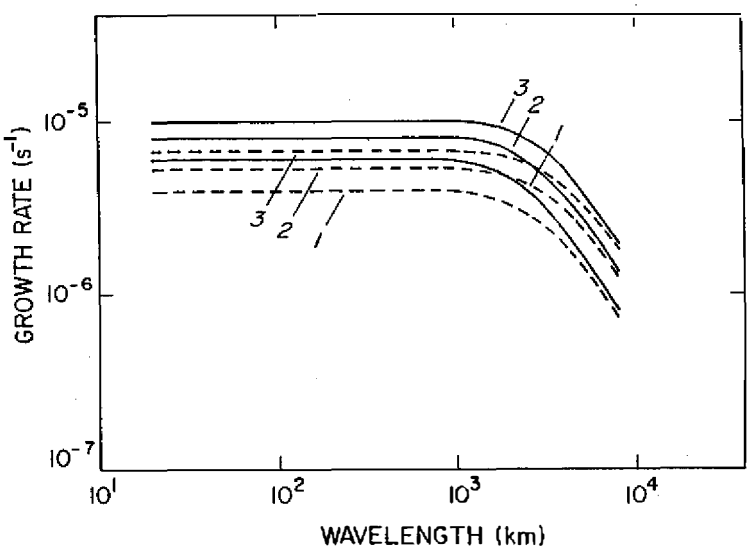

Fig. 2. Same as in Figure 1, but with a smaller heating parameter ε=25 K.

4. NUMERICAL MODEL

A numerical model is used to study the nonlinear feedback mechanism discussed in the introduction section. The model is similar to those used in Chan and Cho (1989), Cho and Chan (1991) and Cho (1993); it is a two dimensional finite difference model in the (X, Z) plane, with central differencing in space and leap frog in time. The model consists of 21 grid points in the vertical and 253 grid points in the horizontal with ΔZ=500 m and ΔX=25 km. Δt=5 min is used in the integration. It is based on (2) through (6), equation (5) is used to determine the vertical velocity for vertical advection and (3) to determine the potential temperature field. The model is solved in the geostrophic domain and results transformed back to the physical space (x, z).

Two sets of integrations are made: one set with no background baroclinic field, and the other with a moderate temperature gradient. In the absence of background baroclinic field, the initial potential vorticity field is given by

$$q = q_0 + q_i \tag{13}$$

with

$$q_0 = f\frac{\partial \bar{\theta}}{\partial Z} \tag{14}$$

where the vertical potential temperature gradient is assumed uniform at the initial time, and

$$q_i = \Delta q_i \exp[-(X - Y_0)^2/L_m^2] \times \begin{cases} 1 - \frac{Z}{Z_q} & Z \le Z_q \\ 0 & Z > Z_q \end{cases} \tag{15}$$

The initial potential temperature field is then

$$\theta = \theta_0 + \frac{q_0}{f}Z + \theta_i \tag{16}$$

where θ_i is determined from (3) with the boundary condition that θ_i=0 at Z=0 and H. Again cumulus heating will be parameterized according to (8) with the piecewise linear heating profile. The condition is applied that heating is zero when w^* is negative.

Figure 3 shows the maxima of vertical velocity over the domain of simulation as functions of time in four different simulations. In the first case (labelled as 1), the value of the potential vorticity anomaly is Δq_i=(1/3)q_0 with L_m=100 km, Y_0=0, and Z_q=3 km. All the other parameters are the same as in the base case of the linear analysis. In case 2, the magnitude of the initial PV anomaly is reduced to $0.1q_0$. In case 3 the eddy viscosity coefficient is reduced by a factor of ten, and case 4 the heating parameter ε is reduced by 1/2. Note that the figure is presented in logarithmic scale, so the rate of increase of the maximum of w is faster than a simple exponential growth. This increase of growth rate is due to the nonlinear feedback process discussed earlier. As the vorticity perturbation is increased, so is the effect of latent heat release. Figure 4 shows the distribution of vertical velocity across the potential vorticity anomaly from the fourth simulation at model time 24 hr. The updraught region which represents the position of the front is only about 250 km wide. Results obtained from the other cases are qualitatively similar.

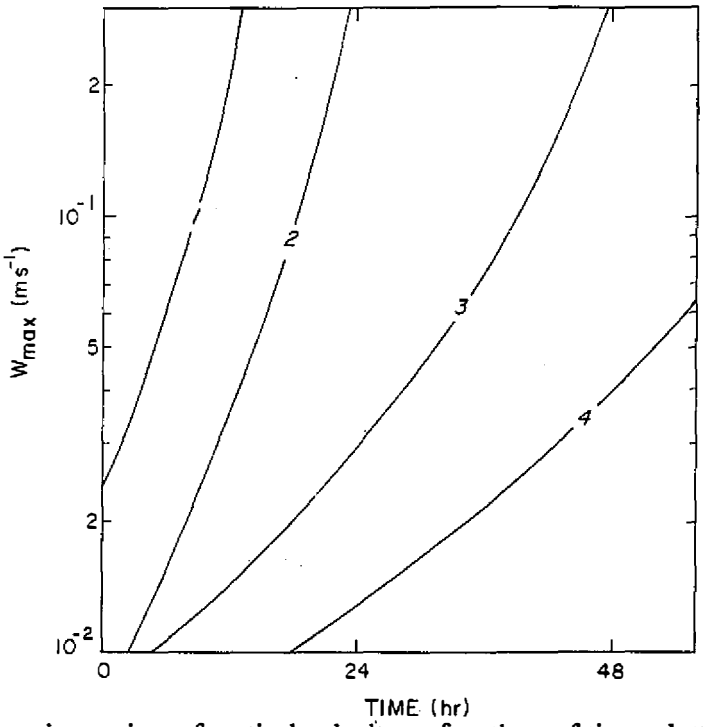

Fig. 3. Domain maxima of vertical velocity as functions of time, plotted in logarithmic scale in four separate simulations. In the base case (1) the potential vorticity perturbation is assumed as $(1/3)q_0$, with L_m=100 km. All other parameters are the same as in the base case of the linear analysis. The other cases are (2) $\Delta q_m=0.1q_0$; (3) K=0.5 m^{2}s^{-1}; and (4) ε=29 K.

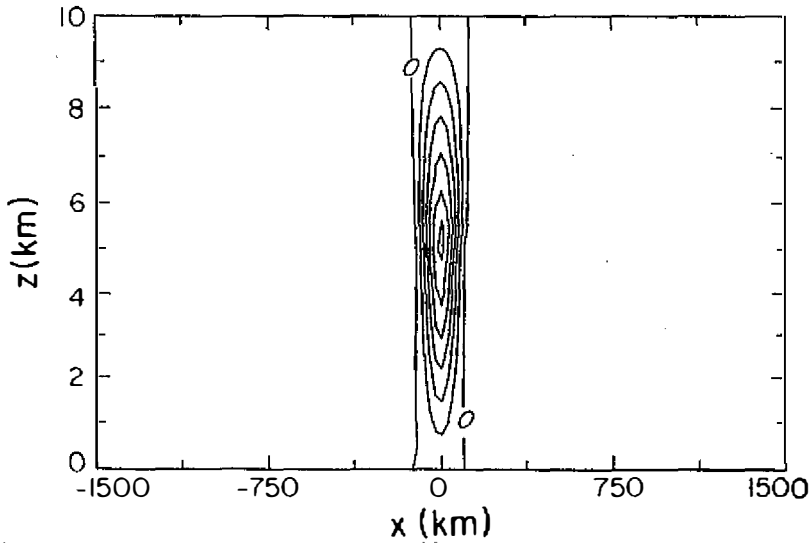

Fig. 4. Distribution of vertical velocity in case (4) at model time 24 hr. Contour intervals are 0.2 cm s^{-1}.

If we consider ther slopes of the curves in Figure 3 as the growth rate, then changing the magnitude of the initial perturbation in q does not have any significant effect on the growth rate. Both the eddy viscosity coefficient and the heating parameter affect the growth rate as indicated by (12), but it is far more sensitive to the value of the heating parameter, as indicated by curves 3 and 4.

In the simulations with a background baroclinic field, again we determine the potential temperature field from (3), but with the following boundary conditions at Z=0, and H:

$$\theta = \theta_0 + \frac{\partial \bar{\theta}}{\partial Z} Z + \theta_s(X) \tag{17}$$

where

$$\theta_s(X) = \Delta\theta_s \quad \tanh(X/L_s) \tag{18}$$

A simulation was made with the following parameter values:

$$\Delta\theta_s = 8K; \quad L_s = 1500km; \quad Y_0 = 1.032L_s; \quad \theta_0 = 289K$$

All other parameters are the same as those in the case shown in Figure 4. The PV anomaly is placed initially at the location where the classical front would form if a frontogenetic forcing is provided at the synoptic scale.

Since there is no large-scale deformation or other type of scale contracting flow imposed on the simulations, the presence of baroclinicity induces no vertical motion whatsoever in the absence of cumulus heating. The only difference it makes is in the background vorticity field associated with the temperature field which, due its effect on the coordinate transformation, tends to give a somewhat larger vertical velocity near the front in physical space. Thus we do not expect any effect other than a somewhat larger vertical velocity and vorticity near the front, especially when one take into consideration the effects of positive feedback of vertical velocity onto itself through cumulus heating.

Figure 5 shows the domain maximum of w, W_{max}, obtained in this simulation in logarithmic scale as a funciton of time (solid curve). Again due to the effect of nonlinear feedback, it grows at a rate faster than that of a simple exponential growth. Compare this with curve 4 in Figure 3, The present case gives a stronger vertical velocity, as explained in the previous paragraph. Also shown in the figure as the dashed curve is the half width of the updraught region at the cloud base level, defined as the width of the region with w>0.5W_{max}, one half of the value of the maximum vertical velocity at the cloud base height. As can be seen from the figure, the half width, and therefore the frontal width, decreases very rapidly as scale contraction due to the convergence flow of the convection continues, even though there is no scale contraction forced onto the system at the synoptic scale. This appears to be the basic mechanism of Mei-Yu frontogenesis. This rapid decrease in horizontal scale is faster than exponential because the self-accelerating nature of the process.

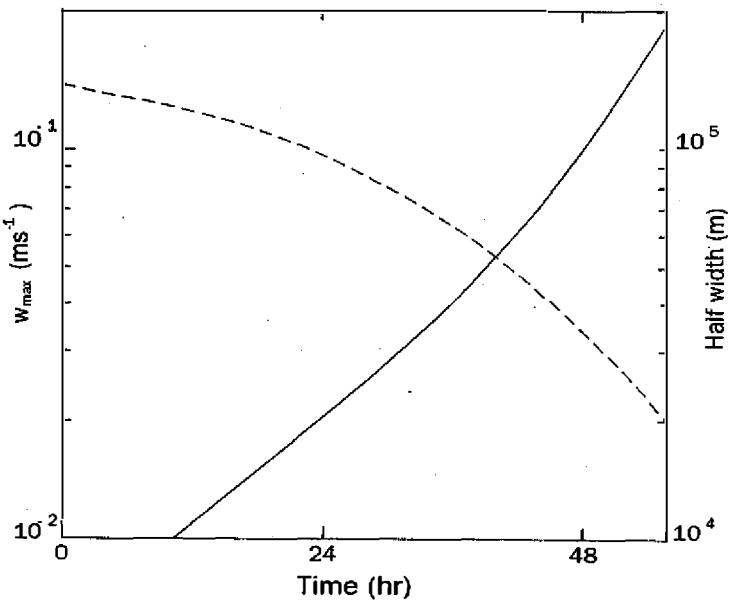

Fig. 5. The variations of W_{max} (solid line) and the half width (dashed line) of updraught at the cloud base level, obtained with a moderate background baroclinicity. See text for the definition of the half width and other details.

5. CONCLUSIONS

The results presented in this paper suggest that Mei-Yu fronts is characterized by a line of high values of low-level potential vorticity which is both the cause and the product of the fronts, and that Mei-Yu frontogenesis is the result of the ageostrophic wind produced by convection along the front.

A linear CISK analysis was first made to illustrate that a front-like structure can be produced from an initially weak perturbation without any synoptic scale forcing. The positive feedback processes responsible for the initial growth is the usual CISK mechanism, that low-level PV anomaly leads to cumulus convection, and cumulus heating further intensifies the low-level PV anomaly. We included in this analysis both the friction-induced low-level convergence as well as the low-level convergence induced by heating, and found the heating induced moisture convergence can be a major fraction of the total convergence responsible for the moisture supply to convection. The intensity of the CISK mechanism is substantially reduced if the heating induced moisture convergence is suppressed.

The linear process, however, is not sufficient by itself to explain the Mei-Yu frontogenesis which is essentially a nonlinear process. We suggest such a nonlinear feedback is provided by the fact that the production of low-level PV by heating is proportional to both the heating and the low-level horizontal wind shear, which in turn is proportional to low-level potential vorticity. A nonlinear numerical model is then used to illustrate the importance of this process. The results of the model showed that due to this process Mei-Yu fronts both intensify and contract in horizontal scale at a rate faster than the exponential rate suggested by the linear CISK theory.

The numerical model used in this first study is by necessity a very simple one. It is expected to be qualitatively correct, but not quantitatively accurate. A better model with a better treatment of the boundary layer processes is needed in future studies.

REFERENCES

Chan, D., S. T., and H. R. Cho, 1989: Meso-β scale potential vorticity anomalies and rainbands. Part I: Adiabatic dynamics of potential vorticity anomalies. *J. Atmos. Sci.*, **46**, 1713-1723.

Charney, J., and A. Eliassen, 1964: On the growth of the hurricane depression. *J. Atmos. Sci.*, **21**, 68-75.

Chen, G. T. J., 1977: A synoptic case study on mean structure of Mei-Yu in Taiwan. *Atmos. Sci.*, **4**, 38-47 (in Chinese with English abstract).

Chen, G. T. J., 1983: Observational aspects of the Mei-Yu phenomena in subtropical China. *J. Meteor. Soc. Japan*, **61**, 306-312.

Chen, G. T. J., 1988: On synoptic-climatological characteristics of the east Asian Mei-Yu front. *Atmos. Sci.*, **16**, 435-446 (in Chinese with English abstract).

Chen, G. T. J., 1990: Overview of Mei-Yu research in Taiwan. East Asia and Western Pacific Meteorology and Climate. P. Shan and C. P. Chang (Eds.), World Scientific Publishing Co., 14-37.

Chen, G. T. J., 1991: Mesoscale features observed in the Taiwan Mei-Yu season. *J. Meteor. Soc. Japan*, **70**, 497-516.

Chen, G. T. J., and C. P. Chang, 1980: The structure and vorticity budget of early summer monsoon trough (Mei-Yu) over southeastern China and Japan. *Mon. Wea. Rev.*, **108**, 942-953.

Chen, G. T. J., and B. J. D. Jou, 1988: Variations of large-scale circulations associated with Mei-Yu fronts of different types. *Atmos. Sci.*, **16**, 309-322 (in Chinese with English abstract).

Chen, G. T. J., and C. Y. Tsay, 1978: A synoptic case study of Mei-Yu near Taiwan. *Papers Meteor. Res.*, **1**, 25-36.

Cho, H. R., and D. S. T. Chan, 1991:Meso-β scale potential vorticity anomalies and rainbands. Part II: Moist model simulations. *J. Atmos. Sci.*, **48**, 331-341.

Cho, H. R., 1993: A mechanism causing mesoscale organizations of precipitation in midlatitude cyclones. *J. Appl. Meteor.*, **32**, 155-160.

Craig, G., and H. R. Cho, 1988: Cumulus heating and CISK in the extratropical atmosphere. Part I: Polar lows and common clouds. *J. Atmos. Sci.*, 2622-2640.

Holton, J. R., 1992: An Introduction to Dynamic Meteorology. 3rd ed., Academic Press. 507pp.

Hoskins, B. J., 1975: The geostrophic momentum approximation and the semi-geostrophic equations. *J. Atmos. Sci.*, **32**, 233-242.

Hoskins, B. J., and F. P. Bretherton, 1972: Atmospheric frontogenesis models: Mathematical formulatin and solution. *J. Atmos. Sci.*, **29**, 11-37.

Kuo, Y. H., and G. T. J. Chen, 1990: Taiwan Area Mesoscale Experiment: An overview. *Bull. Am. Meteor. Soc.*, **71**, 488-503.

Schubert, W. H., and J. J. Hack, 1983: Inertial stability and tropical cyclone development. *J. Atmos. Sci.*, **39**, 1687-1697.

Thorpe, A. J., and C. A. Nash, 1984: Convective and boundary layer parameterizations in a diagnostic model of atmospheric fronts. *Quart. J. Roy. Meteor. Soc.*, **110**, 443-466.

Trier, S. B., D. B. Parsons, and T. J. Matejka, 1990: Observations of a subtropical cold front in a region of complex terrain. *Mon. Wea. Rev.*, **118**, 2449-2470.

Appendix
Comparison of PV Generation by Convective Heating and by Eddy Viscosity

Assuming the Ekman layer model, the vertical velocity at the top of the boundary layer due to eddy viscosity is:

$$w_e^* = \left(\frac{K}{2f}\right)^{1/2} \zeta_r^*$$

For total vertical velocity at the top of boundary layer we assume

$$w^* = \alpha w_e^*$$

Depending on the heating parameter ϵ, a value of 4 would be a reasonable estimate in the mesoscale. Using the heating function given by (8), the rate of PV production due to cumulus heating is estimated:

$$\zeta \frac{\partial E}{\partial Z} \sim \frac{\epsilon}{2Z_p H}\left(\frac{fK}{2}\right)^{1/2} \alpha \zeta_r^* \qquad (A-1)$$

The rate of PV generation due to eddy viscosity can be estimated similarly:

$$K \frac{\partial \theta}{\partial Z} \frac{\partial^2 \zeta}{\partial Z^2} \sim K \frac{\partial \bar{\theta}}{\partial Z} \zeta_r^* \frac{\beta}{D^2} \qquad (A-2)$$

where β is the fraction of the wind shear within the boundary layer that actually takes place above the surface layer; a value β=0.2 will be used in the estimate, D is the boundary layer depth. Using the parameter values in the simulations,

$$[\zeta \frac{\partial E}{\partial Z}]/[K \frac{\partial \theta}{\partial Z} \frac{\partial^2 \zeta}{\partial Z^2}] \sim [\frac{\epsilon}{2Z_p H}][\frac{f}{2K}]^{1/2}[\frac{\partial \bar{\theta}}{\partial Z}]^{-1}[\frac{\alpha}{\beta}] D^2 \sim 40$$

PV generation due to eddy friction is therefore considerably smaller than that due to cumulus heating.